Impacts of soil management and climate on saturated and near-saturated hydraulic conductivity: analyses of the Open Tension-disk Infiltrometer Meta-database (OTIM)

Authors

Guillaume Blanchy[1], Lukas Albrecht[2], Gilberto Bragato[3], Sarah Garré[1], Nicholas Jarvis[4], John Koestel[2,4]

[1]*Flanders Research Institute for Agriculture, Fisheries and Food (ILVO), Melle, Belgium*

[2]*Agroscope, Reckenholzstrasse 191, 8046 Zürich, Switzerland*

[3]*Council for Agricultural Research and Economics (CREA), Via Po, 14, 00198 Roma, Italy*

[4]*Department of Soil and Environment, Swedish University of Agricultural Sciences (SLU), P.O. Box 7014, 750 07 Uppsala, Sweden*

Corresponding author

John Koestel (johannes.koestel@agroscope.admin.ch)

Keywords

hydraulic conductivity, saturated hydraulic conductivity Ks, near-saturated hydraulic conductivity, Kunsat, Knearsat, soil hydraulic properties, infiltration, tension-disk infiltrometer, soil properties, climate, soil, agricultural management practice, pedo-climatic factors, meta-analysis

Abstract

Saturated and near-saturated soil hydraulic conductivities K_h (mm.h^{-1}) determine the partitioning of precipitation into surface runoff and infiltration and are fundamental to soils' susceptibility to preferential flow. Recent studies have found indications that climate factors influence K_h, which is highly relevant in the face of climate change. In this study, we investigated relationships between pedo-climatic factors

26   and K_h and also evaluated effects of land use and soil management. To this end, we collated the Open

27   Tension-disk Infiltrometer Meta-database (OTIM), which contains 1297 individual data entries from 172

28   different publication sources. We analysed a spectrum of saturated and near-saturated hydraulic

29   conductivities at matric potentials between 0 to 100 mm. We found that methodological details like the

30   direction of the wetting sequence or the choice of method for calculating infiltration rates to hydraulic

31   conductivities had a large impact on the results. We therefore restricted ourselves to a subset of 466 of

32   the 1297 data entries with similar methodological approaches. Correlations between K_s and K_h at higher

33   supply tensions decreased especially close to saturation, indicating a different flow mechanism at and

34   very close to saturation as towards the dry end of the investigated tension range. Climate factors were

35   better correlated to topsoil near-saturated hydraulic conductivities at supply tensions ≥ 30 mm than soil

36   texture, bulk density and organic carbon content. We find it most likely that the climate variables are

37   proxies for soil macropore networks created by respective biological activity, pedogenesis and climate

38   specific land use and management choices. Due to incomplete documentation in the source

39   publications of OTIM, we could investigate only a few land use types and agricultural management

40   practices. Land use, tillage system and soil compaction significantly influenced K_h, with effect sizes

41   appearing comparable to the ones of soil texture and soil organic carbon. The data in OTIM show

42   experimental bias is present, introduced by the choice of measurement time relative to soil tillage,

43   experimental design or data evaluation procedures. The establishment of best-practice rules for

44   tension-disk infiltrometer measurements would therefore be helpful. Future studies are needed to

45   investigate how climate shapes soil macropore networks and how land use and management can be

46   adapted to improve soil hydraulic properties. Both tasks require large amounts of new measurement

47   data with improved documentation on soil biology and land use and management history.

1. Introduction

49   Climate models predict more frequent extreme weather events such as high intensity rainfall with the

50   onset of global warming. To prevent water runoff and erosion, soils need to be able to conduct

51   sometimes large amounts of water in a short time. It is generally accepted that one key soil property is

52   the saturated hydraulic conductivity K_s (mm.h^{-1}), as it determines the partitioning of precipitation into

53   surface runoff and infiltration. A large K_s reduces erosion risks and allows water to infiltrate into deeper

54   soil layers, where it may replenish an important reservoir of plant available water or contribute to

55   groundwater recharge. The hydraulic conductivity of a soil decreases with decreasing water content,

56   i.e. with decreasing water saturation. The hydraulic conductivity in the so-called near-saturated range

57   (between 0 and 100 mm matric tensions) is likewise important. Soils with larger near-saturated hydraulic

58   conductivity K_h (mm.h^{-1}) tend to generate less water flow in macropore networks. Therefore, they are

59   less susceptible to preferential flow (Larsbo et al., 2014) by which agrochemicals and other solutes

60   quickly leach towards the groundwater. Moreover, a large K_h also indicates a well-aerated soil, which

61   drains faster and helps air to escape the soil in case of heavy rainfall. This further reduces the risk of

62   surface runoff and erosion as entrapped air strongly decreases soil hydraulic conductivity.

63   Saturated hydraulic conductivity is measured either in the laboratory on small cylinders, usually with

64   diameters < 7 cm (Klute & Dirksen, 1985) or it is acquired from field measurements, either using single

65   or double ring methods (Angulo-Jaramillo et al., 2000). In addition, near-saturated hydraulic

66   conductivities can be measured using a tension disk infiltrometer. The method is designed as a field

67   method, but has been occasionally applied in the laboratory. Using a tension disk infiltrometer, hydraulic

68   conductivities at supply tensions between ca. 0.5 and ca. 60 to 150 mm can be obtained, depending on

69   the specifications of the infiltrometer. All measurement techniques for saturated and near-saturated

70   hydraulic conductivity are laborious, time-consuming and constrained to a relatively small soil volume.

71   It is necessary to develop pedotransfer functions to estimate soil hydraulic conductivities for large-scale

72   modelling applications, as we cannot measure everywhere (Bouma, 1988; Van Looy et al., 2017;

73   Wösten et al., 2001). The development of a pedotransfer function requires a database from which it can

74   be derived. For example, the well-known pedotransfer function ROSETTA (Schaap et al., 2000) is

75   based on the open UNSODA database (Nemes et al., 2001). The equations published in Tóth et al.,

76   2015 are derived from the proprietary EU-HYDI database (Weynants et al., 2013). The pedotransfer

77   functions of Jarvis et al. (2013) are based on an unpublished meta-database containing tension-disk

78   infiltrometer data. Collecting published measurements of saturated and near-saturated hydraulic

79   conductivity measurements into meta-databases and pairing them with other existing databases is

80   essential to develop pedotransfer functions. A notable example is the SWIG database (Rahmati et al.,

81   2018) that collates more than 5000 datasets from soil infiltration measurements, covering the entire

82   globe. Another big effort in collecting information on saturated hydraulic conductivity is the newly

83   published SoilKsatDB (Gupta et al., 2021a), which combines saturated hydraulic conductivity data from

84   several large databases, amongst others UNSODA and SWIG, together with additional measurements

85   published in independent scientific studies. However, none of the databases cited above provide open-

86   access infiltration measurements at tensions near-saturation (h > 0 mm), which limits their use to the

87   estimation of saturated hydraulic conductivity.

88   Pedotransfer functions for saturated hydraulic conductivity exhibit rather poor predictive performance

89   with coefficients of determination R^2 not exceeding 0.25. (Weynants et al., 2009; Jorda et al., 2015).

90   Early approaches, like HYPRES (Wösten et al., 1999) and ROSETTA, focused solely on soil properties

91   like texture, bulk density and organic carbon content. At the time, it was not sufficiently recognized that

92   soil K_s is mostly determined by the morphology of macropore networks, especially in finer-textured soils

93   (Vereecken et al., 2010; Koestel et al., 2018; Schlüter et al., 2020). A pedotransfer function for K_s

94   requires therefore ideally a database that contains direct information on the macropore network itself.

95   But since such measures are even more cumbersome and time-consuming to obtain (e.g. by X-ray

96   tomography) than measuring hydraulic conductivity itself, it is more reasonable and makes more sense

97   to use proxies from which the macrostructure in a soil can be inferred. Ideal candidates would be root

98   growth and the activity of soil macrofauna, which both strongly determine the development of

99   macropore networks in soil (Meurer et al., 2020). However, they are difficult to measure. Proxies that

100   are more promising are land use and farming practises, such as tillage or soil compaction due to

101   trafficking. Plant growth and soil macrofauna in turn are influenced by the local climate. The climate

102   also sets boundaries for the land use and the associated soil management practices, and thus provides

103   feedback to root growth and macro-faunal activity. Wetting and drying cycles and thus the formation

104   and closure of cracks also are regulated by the climate as is splash erosion and soil crusting. It is

105   therefore not surprising that climate variables typically are correlated with saturated and near-saturated

106   hydraulic conductivities (Jarvis et al., 2013; Jorda et al., 2015; Hirmas et al., 2018; Gupta et al., 2021b).

107   Jorda et al., 2015 found that land use itself was the most important predictor for saturated hydraulic

108   conductivity.

109   The time of measurement of the hydraulic conductivity (or soil sampling) also has a crucial impact. In

110   an agricultural soil, the hydraulic properties of a freshly prepared seedbed differ from those measured

111   later at harvest. Several studies have demonstrated the evolution of hydraulic conductivity with time

112   (Messing & Jarvis, 1990; Messing and Jarvis, 1993; Bodner et al., 2013; Sandin et al., 2017). Soil

113   management options (such as tillage or the use of cover crops) actively influence the soil saturated and

114   near-saturated hydraulic conductivity. Information on their impact is therefore especially important, but

115   so far has hardly been investigated in meta-studies.

116   In this study, we quantified the effect of soil management practices on soil saturated and near-saturated

117   hydraulic conductivity, K_h. We also compared the strengths of relationships between K_h and soil

118   management practices and other potentially important influencing factors like soil properties, local

119   climate and details of the measurement methods. In this process, we expanded and published the

120   previously unpublished meta-database on tension-disk infiltration measurements that was first reported

121   by Jarvis et al. (2013). We referred to this database as OTIM in the following (Open Tension-disk

122   Infiltrometer Meta-Database). It complements the currently available public databases on hydraulic

123   conductivities, which are strongly based on laboratory measurements or ring infiltrometer methods.

2   Material and Methods

2.1   Meta-Database, OTIM

2.1.1   Data collection

127   The first version of OTIM was compiled for the study by Jarvis et al., 2013. The original database

128   contained 753 tension-disk infiltrometer data entries collated from 124 source publications, covering

129   144 different locations around the globe. We have extended this database by 544 new tension-disk

130   infiltrometer data entries from 48 additional studies that had been published after 2012. The search for

131   publications was carried out between 2021-05-31 and 2021-06-23 using the queries and search engines

132   detailed in Table A1.

133   We found 115 publications containing tension-disk infiltrometer measurements published in 2013 or

134   later. We retained the data for further analysis when (i) K_h or the infiltration rate was measured at more

135   than two tensions larger or equal to 5 mm and (ii) sufficient meta-data on soil and site properties (at

136   least soil texture) as well as soil management practices (at least land use and tillage) were available. If

137   a publication only reported infiltration rates, we calculated hydraulic conductivity using the method of

138   Ankeny et al. (1991). Only 45 of the 115 publications fulfilled the above-mentioned criteria. Table A2

139   summarises how many papers were rejected and for which reasons. For 27 of the 45 retained studies,

140   we digitised the published K_h values from figures using WebPlotDigitizer (open-source web-based

141   software created by Ankit Rohatgi, https://automeris.io/WebPlotDigitizer/). For cases in which K_h

142   measurements were mentioned in a publication, but the results were not reported, we contacted the

143   corresponding authors. We received the data in this fashion for three of these publications (Alletto et

144   al., 2015; Larsbo et al., 2016a; Meshgi & Chui, 2013). The new studies containing data added to the

145   OTIM database are summarised in Table 1.

146   **Table 1: List of new entries added to the Jarvis et al., 2013 database.**

Reference	Land use	Tillage	Compaction	Sampling time	Data entries
Alagna et al., 2015	grassland	no tillage	not compacted	consolidated soil	1
Alletto et al., 2015	arable	conventional tillage	unknown	consolidated soil	60
Bagarello et al., 2014	arable	no tillage | conventional tillage	unknown	unknown	10
Baranian Kabir et al., 2020	grassland | arable	no tillage	not compacted | compacted	unknown | consolidated soil	4

Báťková et al., 2020	arable	reduced tillage | no tillage | conventional tillage	unknown	consolidated soil | soon after tillage	12
Bodner et al., 2013	arable	no tillage	unknown	soon after tillage | consolidated soil	12
Bottinelli et al., 2013	arable	unknown | conventional tillage | reduced tillage | no tillage	unknown	consolidated soil	10
Costa et al., 2015	arable	conventional tillage | reduced tillage | no tillage	not compacted	consolidated soil	3
De Boever et al., 2016	grassland	no tillage	not compacted	unknown	6
Tóth et al., 2014	arable	conventional tillage	not compacted | compacted	consolidated soil	2
Etana et al., 2013	arable	conventional tillage	not compacted | compacted	unknown	2
Fashi et al., 2018	arable	no tillage | reduced tillage | conventional tillage	compacted | not compacted	unknown	8

Fasinmirin et al., 2018	arable | woodland/plantation | grassland	conventional tillage | no tillage	not compacted | compacted	unknown	3
Greenwood, 2016	arable | grassland	conventional tillage | no tillage	unknown	consolidated soil	4
Hallam et al., 2020	arable	conventional tillage	not compacted	unknown	60
Hardie et al., 2012	arable	no tillage	not compacted	consolidated soil	2
Holden et al., 2014	grassland	no tillage	not compacted	consolidated soil	5
Hyväluoma et al., 2019	arable	conventional tillage	unknown	consolidated soil	4
Iovino et al., 2016	arable | grassland | woodland/orchard	reduced tillage | no tillage	unknown	consolidated soil	3
Kelishadi et al., 2013	arable | grassland	reduced tillage | no tillage | conventional tillage	not compacted	consolidated soil	4
Keskinen et al., 2019	arable	no tillage | conventional tillage	unknown	consolidated soil	15

Khetdan et al., 2017	arable	no tillage	unknown	unknown	4
Larsbo et al., 2016a	arable	conventional tillage	not compacted | compacted	consolidated soil | unknown	5
Lopes et al., 2020	woodland/orchard | grassland	no tillage	not compacted	consolidated soil	4
Lozano et al., 2014	arable	no tillage	not compacted	consolidated soil	2
Lozano-Baez et al., 2020	grassland | woodland/orchard	no tillage	not compacted	unknown	18
Matula et al., 2014	grassland	no tillage	unknown	unknown	3
Miller et al., 2018	arable	conventional tillage	unknown	consolidated soil	10
Mirzavand, 2016	arable	conventional tillage | reduced tillage | no tillage	unknown	consolidated soil	12
Pulido Moncada et al., 2014	arable | grassland	conventional tillage | no tillage	unknown	unknown	4
Rahbeh, 2019	arable	conventional tillage	unknown	consolidated soil	69

Rienzner & Gandolfi, 2013	arable	conventional tillage	not compacted	unknown | consolidated soil	18
Sandin et al., 2017	arable	conventional tillage	not compacted | compacted	consolidated soil | unknown	7
Soracco et al., 2015	grassland	conventional tillage	not compacted | compacted	unknown	3
Soracco et al., 2019	arable	conventional tillage | no tillage	unknown	consolidated soil	6
Wang, 2021	arable	conventional tillage	unknown	soon after tillage | consolidated soil	25
Wanniarachchi et al., 2019	arable	conventional tillage	unknown	consolidated soil	6
Yu et al., 2013	grassland	no tillage	unknown	unknown	11
Yusuf et al., 2017	arable	no tillage	not compacted	consolidated soil	1
Yusuf et al., 2020	arable	no tillage	not compacted	consolidated soil	5
Zeng et al., 2013	woodland/orchard	conventional tillage	unknown	consolidated soil	20

Zeng et al., 2012	grassland	no tillage	unknown	consolidated soil	6
Zhang et al., 2013	grassland | arable	no tillage | unknown	unknown	consolidated soil	6
Zhang et al., 2014	arable	conventional tillage	unknown	consolidated soil	4
Zhang et al., 2016	woodland/orchard | arable	no tillage | conventional tillage	unknown | not compacted	consolidated soil | soon after tillage	24
Zhang et al., 2021	grassland | woodland/orchard | arable	no tillage | conventional tillage	unknown	consolidated soil	4
Zhao et al., 2014	arable | grassland	conventional tillage | no tillage	not compacted	unknown	12
Zhou et al., 2015	arable | grassland | woodland/orchard	conventional tillage | no tillage	not compacted	soon after tillage	3

147

148 In addition to adding data from new publications to OTIM, we also revisited the studies contained in the

149 original version of the database and collected additional information on soil management practices

150 associated with the measured data. For each soil management option, OTIM contains two columns. In

151 the first column, the information as given in the source publication is stored. The second column

152 summarises this information into a few classes, which were subsequently used in the meta-analysis. In

153 this study, we investigated effects of land use, tillage system, soil compaction and day of measurement

154   relative to the latest tillage operation on the field. A compaction class was assigned to a data entry only

155   if the plot had been described as 'compacted' or 'not compacted' in the source publication. 'Compacted'

156   data entries corresponded, for example, to infiltration measurements in wheel tracks or on plots of a

157   compaction experiment. The day of measurement relative to tillage was also included, with the data

158   labelled 'freshly tilled' when the authors in the source publication stated that the measurements had

159   taken place soon after tillage. Otherwise, it was assumed that the soil had already had time to

160   consolidate before the infiltration measurements were carried out. All soil texture data was mapped

161   onto the USDA classification system using the method proposed in Nemes et al. (2000).

162   ### 2.1.2.   Climate data and soil classification

163   The climatic data entries provided in the database were created using the bioclimatic raster data

164   (BioClim) provided by WorldClim (worldclim.org). The data was averaged across the years 1970 to

165   2000 and had a 30 arc second resolution (~1 km^2; Fick & Hijmans, 2017). The available climate

166   variables were mean annual temperature and precipitation, the mean temperature as well as mean

167   precipitation of the warmest, coldest, wettest and driest quarter and month, respectively, the

168   isothermality, the mean diurnal and annual temperature range, the seasonality for temperature and

169   precipitation. Besides the bio-climatic data in WorldClim we included the aridity index (here defined as

170   the annual precipitation divided by the potential evapotranspiration) as well as the average annual

171   potential evapotranspiration (ET_0). Both were inferred from the "Global Aridity Index and Potential

172   Evapotranspiration Climate Database v2" that is based on the WorldClim database (Trabucco & Zomer,

173   2019). The World Reference Base (WRB) soil type was also extracted from the source publications.

174   When it was not reported, the SoilGrids database by ISRIC (Poggio et al., 2021) was used to infer it.

175   The map contained information about the main soil type regarding the WRB classes (IUSS Working

176   Group WRB, 2015). The most probable soil type was chosen for each location. For all discussed climate

177   and soil maps, the python package "rasterio" (v1.2.10) was used to collect the variables from the

178   corresponding raster cell at the location coordinates given in the source publications.

179   ### 2.1.3   Model fit to infer K_h at near-saturated tensions not measured

180   Tension-disk infiltrometers measure infiltration rates at a specific supply tension (Angulo-Jaramillo et

181   al., 2000). They consist of a ceramic disk to which a water reservoir and a bubbling tower is attached.

182   The ceramic disk is saturated and hydraulically connected to the soil by inserting a layer of fine sand

183   between the disk and the soil surface. The supply tension at the bottom of the ceramic disk is adjusted

184   by the bubbling tower. The measured unconfined (i.e. three-dimensional) infiltration rates are then

185   commonly converted to hydraulic conductivities with the aid of the Wooding equation (Wooding, 1968).

186   Note that unconfined tension-disk infiltrometers cannot provide measurements at a tension of zero, i.e.

187   K_s. Even if many publications report K_s values obtained from tension-disk infiltrometers, these

188   measurements must have been conducted at tensions slightly larger than zero, as water would

189   otherwise have freely leaked out of the tension disk. For this reason, we set the tensions for K_s

190   measurements to 1 mm, but still referred to these data as saturated hydraulic conductivity.

191
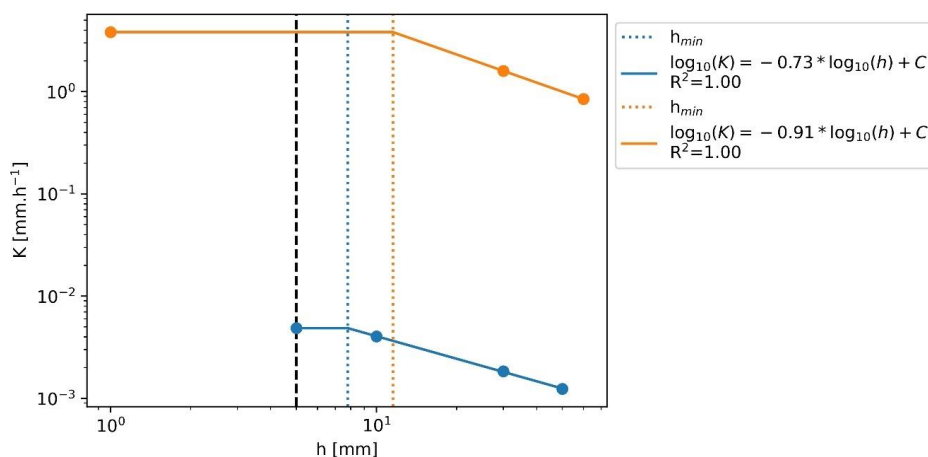
Figure 1: Example of linear fit in log-space. K_s values were assigned a tension of 1 mm for illustration purposes. The equations for the linear part of the fit are shown in the legend. C represents the intercept with the y-axis of the linear fit in log-space, h_{min} corresponds to the supply tension at which the largest pores in the soil are water-filled.

196   Following Jarvis et al., 2013, we interpolated K_h for tensions in-between the ones measured in the

197   source publications. We achieved this by fitting a log-log linear model with a kink at a tension h_{min}, which

198   denotes the tension at which the largest effective pores in the soil are water-filled (see Figure 1).

199   Therefore, $K_h == K_s$ for all tensions h ≤ h_{min}. If K_s was not measured but instead a K_h value at h ≤ 5 mm

200   was available, K_s was set to the available K_h value (Figure 1 orange line). In cases where more than

201   one K_h value was measured at a tension smaller or equal to 5 mm (including h = 0 mm, i.e. K_s), we

202   averaged them and fixed K_s and K_h for h ≤ h_{min} to the average (Figure 1 green line). K_h values at h > 5

203   mm were used to fit the log-log linear relationship. The tension at which the fitted log-log slope

204   intersected with Ks defined h_{min}. We used the fitted model to estimate all K_h values for tensions for 10

205   ≤ h ≤ 100 mm at 10 mm intervals. The K_h values were only interpolated between the tensions that were

206   measured in the source publication. The only exceptions from this rule were made in the case where a

207   K_h value for a tension of 80 or 90 mm was provided together with at least one other K_h value measured

208   at a smaller tension. Then, the missing K_h values were extrapolated up to a tension of 100 mm. Figure

209   1 shows examples of model fits. Only entries with an R^2 greater or equal to 0.9 were retained in the

210   analysis.

211   ## 2.2   Data availability and spatial coverage

212   Although 92% of the OTIM data is from the topsoil, it also contains some data points measured at

213   greater soil depths. In the following meta-analysis, only measurements from the topsoil were included

214   to prevent bias and all datasets measured at soil depths below 200 mm were removed. Last but not

215   least, we found that the relationship between supply tension and K_h was distorted if data entries were

216   included that did not cover the complete tension range from h = 0 to 100 mm. Possible reasons for the

217   difficulties to match K_h data from tension series with different lengths are discussed at the beginning of

218   the results and discussion section. Otherwise, we focused on data entries that included K_h values for

219   the complete tension range in the exploratory data analysis and the meta-analyses. The available

220   datasets after these filtering steps correspond to the ones indicated in blue (and termed 'focus') in the

221   following figures.

222   Most tension-disk infiltrometer studies were conducted in Europe, North America and Southeast

223   Australia (Figure 2). Clearly, fewer studies have been carried out in Asia, South America and Africa.

224   The lack of datasets from Russia, Mesoamerica, the arctic regions and the tropics is remarkable. This

225   geographical bias is aggravated if only measurements on the topsoil are considered that allow

226   inferences about K_h for the complete range of tensions (0 ≤ h ≤ 100 mm) with a sufficiently good

227   coefficient of determination. Then, all the data entries collected in southern South America and south-

228   eastern Australia were omitted, as well. Overall, the data in OTIM mostly stem from temperate climate

229   regions.

230
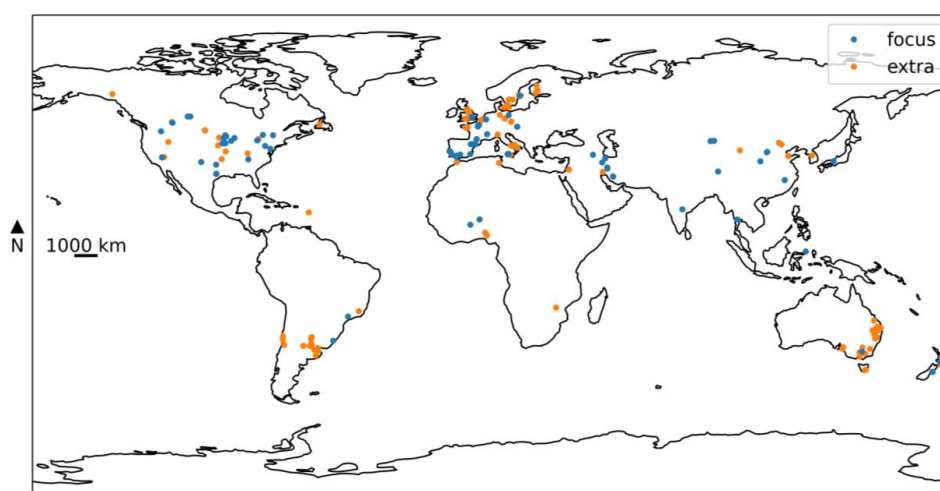
Figure 2: Map of the study locations collected in the OTIM. The values are shown for the

filtered entries ('focus') and in parenthesis for all the entries available in the database

('focus' and 'extra').

234   Figure 3 depicts the number of K_h values available for 0 ≤ h ≤ 100 mm. These figures represent the

235   hydraulic conductivities derived from the log-log linear model presented above, not the raw data

236   measured and reported in the source publications. A large number of entries span the full range of

237   tensions of interest (0 to 100 mm), whereas a smaller number of entries only have data up to a tension

238   of 60 mm. Often, but not always, such data series were obtained with the widely available Mini-Disk

239   infiltrometer distributed by the *Meter* group (formerly by *Decagon*), which is limited to tensions h ≤ 70

240   mm. An overview on the metadata included in OTIM is given in Table 2. Data gaps are present,

241   especially for bulk density and for information on the soil management at the study site, apart from

242   tillage operations. Note that the annual mean temperature and precipitation are only two examples

243   representing the climatic variables enumerated in section 2.3. There are very few missing values for

244   the climate data, since it was estimated from the coordinates of the study sites. The same holds for the

245   elevation data and information on the WRB soil type.

246   **Table 2: Number of entries and gaps for each feature along with units and range (if**
247   **continuous) or choices (if categorical). The values are shown for the filtered entries**
248   **('focus') and in parenthesis for all the entries available in the database ('focus' and 'extra').**

Type	Predictor	Unit	Range/Choices	Number of entries	Number of gaps
Soil	Sand content	kg kg^{-1}	0.0 -> 0.9 (0.0 -> 1.0)	402 (1070)	64 (215)
Soil	Silt content	kg kg^{-1}	0.0 -> 0.8 (0.0 -> 0.8)	402 (1070)	64 (215)
Soil	Clay content	kg kg^{-1}	0.0 -> 0.7 (0.0 -> 0.8)	405 (1107)	61 (178)
Soil	Bulk density	g cm-3	0.5 -> 1.8 (0.1 -> 2.2)	324 (771)	142 (514)
Soil	Soil organic carbon	kg kg^{-1}	0.0 -> 0.1 (0.0 -> 1.0)	339 (938)	127 (347)
Climate	Annual mean temperature	°C	-0.4 -> 29.1 (-3.8 -> 29.1)	466 (1214)	0 (71)
Climate	Annual mean precipitation	mm	22.0 -> 3183.0 (22.0 -> 3183.0)	466 (1214)	0 (71)
Climate	Average aridity index	-	0.0 -> 1.9 (0.0 -> 2.8)	466 (1214)	0 (71)
Climate	Precipitation seasonality (CV)	-	9.9 -> 138.5 (9.6 -> 138.5)	466 (1214)	0 (71)
Climate	Mean diurnal range	ºC	6.9 -> 18.2 (4.8 -> 18.5)	466 (1214)	0 (71)
Management	Land use	-	arable, bare, grassland, woodland/plantation	453 (1249)	13 (36)
Management	Tillage	-	conventional tillage, no tillage, reduced tillage	422 (1190)	44 (95)
Management	Soil compaction	-	compacted, not compacted	76 (265)	390 (1020)
Management	Sampling time	-	soon after tillage, consolidated soil	367 (993)	99 (292)

249
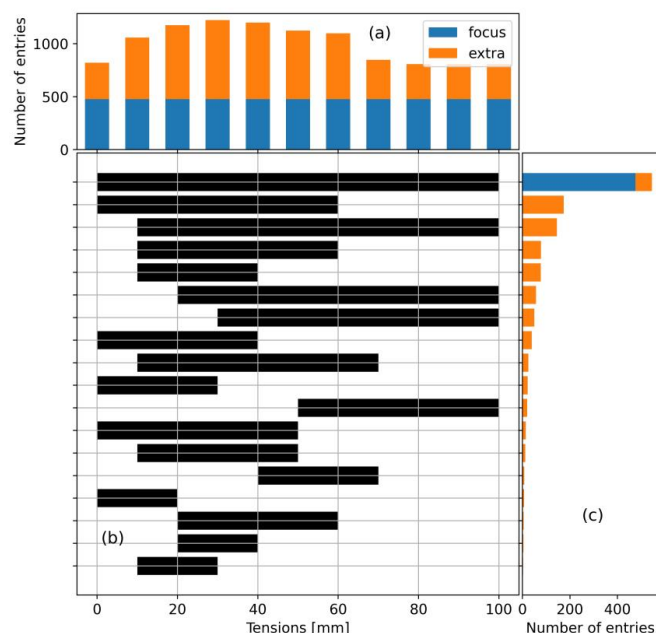
Figure 3: (a) number of available K_h values per supply tension, (b) range of available tensions and (c) their respective occurrence in the database. The values are shown for the filtered entries ('focus') and in parenthesis for all the entries available in the database ('focus' and 'extra').

just blue and orange !

The metadata for the datasets used in the exploratory data analysis are summarized in Figure 4. OTIM

contains predominantly data from arable fields. The distributions of the climate variables confirms that

the data in OTIM was also mostly acquired in temperate climates, with a bias towards the somewhat

drier climates that are most typical for arable land. The soil texture, bulk density and organic carbon

content data also appear reasonably representative for soils in this climate zone.

260
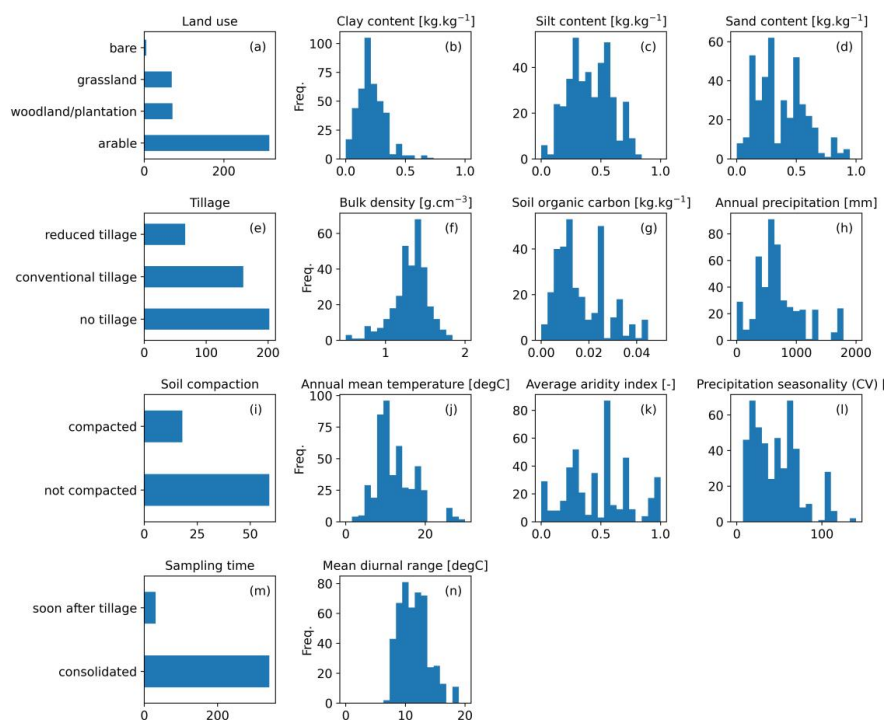
Figure 4: Distributions of continuous and categorical variables in the 'focus' dataset.

2.3 Exploratory data analysis

Some source publications only provided a few data entries for K_h, sometimes only comparing two different treatments, while other source studies contain data for a larger number of treatments and/or sites. In some publications, data for all individual tension-disk measurements are available, even if replicates were measured. In others, only averages of the replicated measurements are reported, while still others yield average K_h values for individual replicated treatment blocks. This makes appropriate data weighting complicated, but also extremely important when analysing the meta-dataset. It also introduces uncertainty, because it is not always clear whether the replicated averages were calculated using the geometric or the arithmetic mean. Considering that hydraulic conductivities at or near saturation are known to be log-normally distributed, the former would be best. In the following, we

272   assumed that geometric averaging was used when replicated values were reported in source

273   publications. In the following, we calculated data weights as

274                          $$\omega_i = \frac{n_{r,i}}{\sqrt{N_i}}$$ Equation 1

275   where ω_i is the weight for data entry i, $n_{r,i}$ is the number of replicates from which the values of i were

276   averaged and N_i is the total number of measurements included in the publication from which data entry

277   i was obtained. With this approach, we up-weighted data entries according to the number of replicate

278   measurements from which they were averaged and down-weighted the impact of studies that published

279   larger amounts of data.

280   We used weighted Spearman rank correlation coefficients to investigate relationships between

281   continuous variables. We considered correlations significant if they exhibited p-values of less than 0.05.

282   The latter were determined numerically by running randomization tests with 200 repetitions.

283   2.4   Meta-analysis

284   Data entries in OTIM with specific land use or management were very unevenly distributed. For

285   example, the large majority of data was measured on sites with land use 'arable' (see Figure 4a). Such

286   uneven distributions may lead to bias when averaged over all entries of a specific feature in exploratory

287   data analyses. We therefore investigated the effects of land use and management as well as soil

288   compaction and time of measurement on K_h with the aid of pairwise comparisons published within

289   individual studies and calculated effect sizes (ES) for each investigated class.

290   To reduce bias arising from the varying number of data entries published within individual studies, we

291   grouped all entries according to the factors land use, tillage, compaction, and sampling time. Here we

292   only considered binary pairs, that is arable or not arable in the case of land use and tilled or not tilled,

293   compacted or not compacted as well as 'measured soon after tillage' or 'measured on consolidated soil'

294   for the other three factors. In addition, we checked whether different entries within individual studies

295   stemmed from the same or a very similar site. We did this by comparing the respective USDA texture

296   classes and a climate variable, namely the aridity class. All data entries within each individual study that

297 exhibited identical land use, soil management, soil compaction, sampling time, texture and aridity were

298 averaged and the number of corresponding replicates was summed.

299 For each binarized factor (e.g. tillage), a *control* value was chosen (e.g. zero tillage). All values different

300 from the control represent the *treatment* (e.g. conventional tillage and reduced tillage). Within individual

301 studies, pairs among the averaged entries were formed for each combination of a control and a

302 treatment value. These pairs were used to compute the effect size. Following Basche & DeLonge

303 (2019), we defined the effect sizes as the log10 of the ratio of $K_{h,t}$ of the treatment divided by $K_{h,c}$ of the

304 control

305 $$ES_l \; = \; log_{10}\left(\frac{K_{h,t}}{K_{h,c}}\right)$$ Equation 2

306 where the subscript l indicates the lth pair for which the effect size was computed and the indices 't' and

307 'c' stand for treatment and control, respectively. The average effect size *ES* for each of the four

308 investigated factors was calculated as the weighted mean of the individual ES_l using the weight

309 $$w_l = \frac{v_c \, v_t}{v_c + v_t}$$ Equation 3

310 where the subscript l indicates again the lth pair for which the effect size was computed and v_c and v_t

311 denote the number of (summed) replicates for control and treatment, respectively. In addition, we

312 calculated the weighted standard error

313 $$\sigma_{\bar{ES}} = \sqrt{\frac{\sum_{l=0}^{n} \; w_l \left(ES_l - \overline{ES}\right)^2}{\frac{n-1}{n}\sum_{l=0}^{n} \; w_l}}$$ Equation 4

314 where $\overline{ES}$ is the mean effect size. Table 3 summarises the evaluated factors, the number of pairs

315 involved and the number of different studies from which the pairs were obtained.

316 To estimate the robustness of the effect size, we carried out a sensitivity analysis using the Jackknife

317 technique, similarly to Basche & DeLonge, 2019. This method aims to show the sensitivity of the

318 averaged effect size to data from specific studies. For each factor, a given number of studies was

319 randomly picked and removed from the dataset. The averaged effect size and its standard error was

320 computed with the rest of the dataset. The process started by removing one study, after which up to

321 nine more studies were removed. This random selection was repeated 50 times to rule out bias. The

322 average of the means and standard errors for the 50 realisations was computed and plotted. Observed

323 effect sizes were judged trustworthy if they did not change after removal of studies to calculate

324 them. We constrained the sensitivity analyses in our study to the effect sizes for K_s and K_{100}. *should be introduced!*

325 **Table 3: Number of studies and paired comparison with their respective control and**
326 **treatment values used for the meta-analysis exemplary for the K_{100} values.**

Factor	Control	Treatments	Studies	Paired comparisons
Land use	not arable	arable	10	24
Tillage	no tillage	conventional tillage, reduced tillage	15	32
Compaction	not compacted	compacted	6	8
Sampling Time	consolidated soil	soon after tillage	6	12

327

3 Results and discussion

3.1 Differences between data entries with different tension ranges

330 If all data are considered ('focus' and 'extra'), Figure 3 illustrates that approximately 40% of the data in

331 OTIM provided K_h for every (h) with 0 ≤ h ≤ 100 mm. For another 40%, K_h was only measured in the wet *italic above?*

332 range, i.e. at tensions below 70 mm. The remaining K_h data was only acquired at the dry range. Here,

333 we counted all data entries for which K_s were not measured and could not be estimated. Figure 5 shows

334   how data from entries with complete, dry and wet ranges differed. The K_h for the wet range receded

335   faster with increasing tension than series that also included measurement in the dry range. A large

336   portion of these datasets were obtained with the Mini-Disk infiltrometer. However, a closer inspection

337   of the impact of the disk diameters used to acquire the respective K_h did not confirm suspicions that the

338   bias was related to the use of this special type of infiltrometer (see Figure 6a). The observed differences

339   between the K_h curves could have been introduced by co-correlations with soil texture or climate.

340   Another explanation may be experimenter bias, since individual research groups tend to use specific

341   tension ranges for more than one study. In this study, however, we focused solely on data entries for

342   which we were able to reconstruct K_h for all h in between 0 and 100 mm supply tension in the following

343   exploratory data analyses and meta-analyses. This greatly facilitated the data interpretation.
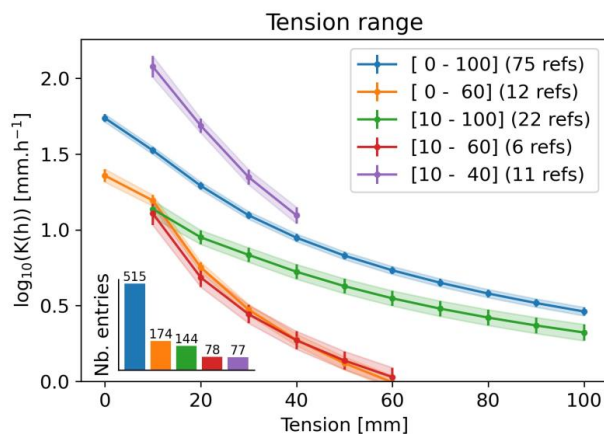
344

345   **Figure 5: Evolution of weighted mean K_h with tension available in OTIM, sorted by the**
346   **tension range the data was spanning. The number of publications from which the data**
347   **originated is shown between parentheses in the legend. The shaded areas and the error**
348   **bars represent the weighted standard error of the mean.**

349   3.2   Statistical relationships between K_h and methods used

350   Figure 6a confirms that the diameter of the tension disk did not have a systematic impact on the results.

351   The majority of the data were collected starting under dry conditions (large tensions) and subsequently

352   measured under increasingly wet conditions (smaller tensions). Figure 6b illustrates that beginning the

353   experiment under wet conditions is associated with larger hydraulic conductivities at identical supply

354   tensions. This is well known and is referred to as hysteresis, which is due to ink-bottle effects, impacts

355   of water repellency, air entrapment and swelling of clay particles (Hillel, 2004). Figure 6c shows that the

356   large majority of studies used the 'steady-state piecewise' method to solve the Wooding equation and

357   convert the measured infiltration rates to hydraulic conductivities. This method leads to smaller K_h for

358   larger tensions than the other methods. The 'transient' and 'steady-state constant' methods yielded

359   larger K_h in the unsaturated range. For the latter method, it is known that it overestimates unsaturated

360   K_h (Jarvis et al., 2013). We tested whether excluding data from 'transient' and 'steady-state constant'

361   methods changed the results of the meta-analyses, but found that they only changed to a minor degree.

362   Data from all methods were therefore included in the following. Note that the 'transient' method was

363   mostly applied in conjunction with Mini-Disk Infiltrometers, albeit the respective data is not included in

364   Figure 6 since it does not span the entire suction range.
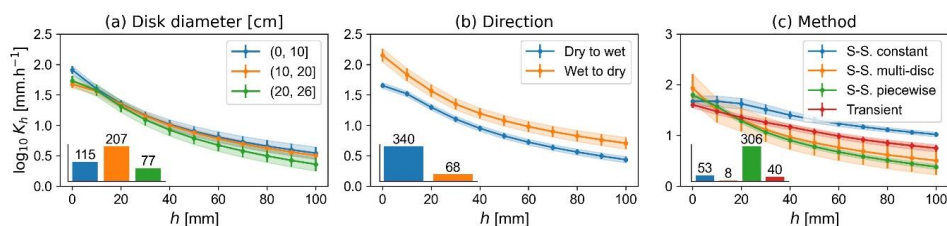
365

366   **Figure 6: Evolution of weighted mean K_h as a function of applied tension for (a) disk**
367   **diameter, (b) direction and (c) method of fitting. 'S.-S.' stands for 'steady-state'. More**
368   **specifically, the method 'S.-S. constant' is outlined in Logsdon and Jaynes (1993), 'S.-S.**
369   **multi-disc' in Smettem and Clothier (1989), and 'S.-S. piece-wise' in Reynolds and Elrick**
370   **(1991) or Ankeny et al. (1991) and 'Transient' in Zhang (1997) or Vandervaere et al. (2000).**
371   **The shaded areas and the error bars represent the weighted standard error of the**
372   **mean.The bar plots in each subplot indicate how many data points of each class were in**
373   **the data set.**

374   3.3   Correlation between K_h at different tensions

375   The fact that correlations between K_h estimated at supply tensions between 40 and 100 mm were

376   relatively stable (Table 4) indicates that the respective flow paths and/or mechanisms remained very

377   similar in this tension range. However, these correlations weakened at tensions between 10 and 20

378   mm, giving rise to the existence of a threshold above which water flow in the largest macropores

379   becomes the dominant flow mechanism. The poor correlation between K_s and K_h at larger supply

same here

380 tensions is in line with findings that K_s is not well suited to infer to soil unsaturated hydraulic

381 conductivities (Schaap and Leij, 2000).

382
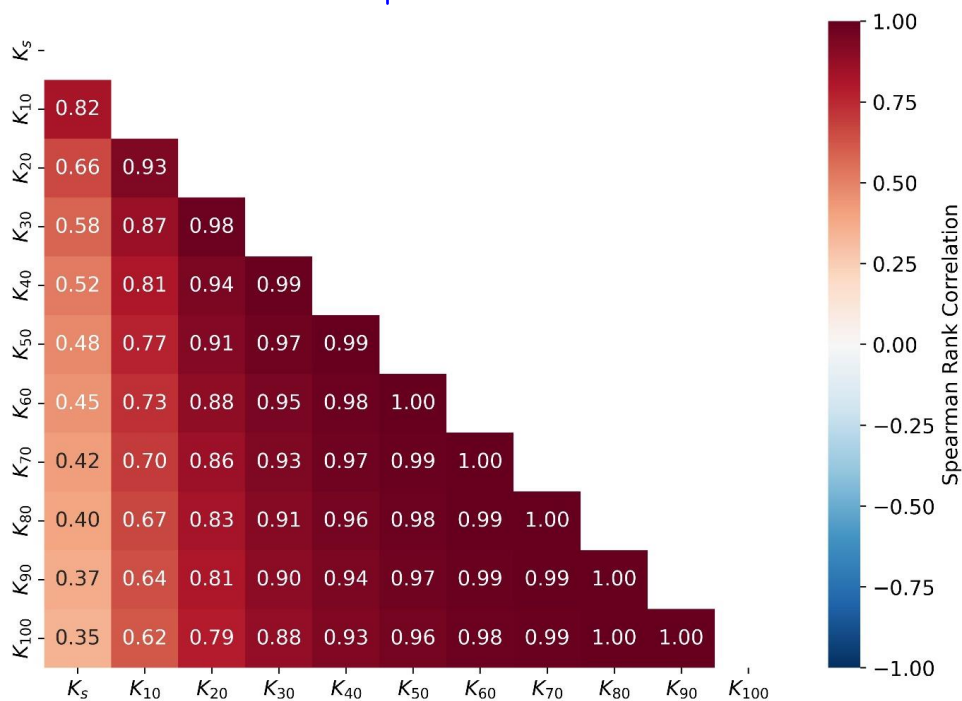
Table 4: Weighted Spearman rank correlation coefficients between K_h at different tensions.

Correlation coefficients are shown up to p-values of 0.001.

385 ### 3.4 Statistical relationships between K_h and soil properties

386 Soils with coarse texture exhibited larger K_h in the unsaturated range, which is caused by the large and

387 abundant primary pores in between individual sand grains (Figure 7a). At saturation, the average

388 hydraulic conductivity of all three texture classes was similar. This is explained by the presence of large

389 structural pores in the medium and fine-textured soils. Medium-textured soils had the lowest K_h in the

390 investigated range of tensions, which may be due to a denser soil matrix in loamy soils and a lower

391 structural stability of silty soils. Larger bulk densities decreased K_h across the whole range of

392 investigated tensions, which reflects the reduced porosity with increasing bulk density (Figure 7b).

393 The hydraulic conductivity in the saturated and near-saturated range is especially affected by soil

394 compaction, which predominantly reduces the abundance and connectivity of macropores (Pagliai et

395 al., 2004; Whalley et al., 1995). Large bulk densities are also known to reduce burrowing activities of

396 the soil macrofauna (Capowiez et al., 2021) as well as root growth (Lipiec & Hatano, 2003), also leading

397 to less abundant and less connected large macropores. An increase in the soil organic carbon content

398 was connected with smaller K_h at the dry end of the investigated tension range if soils with organic

399 carbon contents of more than 0.03 kg.kg^{-1} were excluded (Figure 7c). This decrease may be explained

400 by water repellency, which is generally positively correlated with organic carbon content. A similar

401 observation was already reported in Jarvis et al. (2013). Note that no major correlations of SOC with soil

402 texture were observed in the investigated dataset (Table 5). For soils with organic carbon contents

403 larger than 0.03 kg.kg^{-1}, K_h increased once again. This may indicate that, above this threshold, better-

404 developed macropore networks associated with large SOC contents (e.g. Larsbo et al., 2016b)

405 outweighed any effects of water repellency.
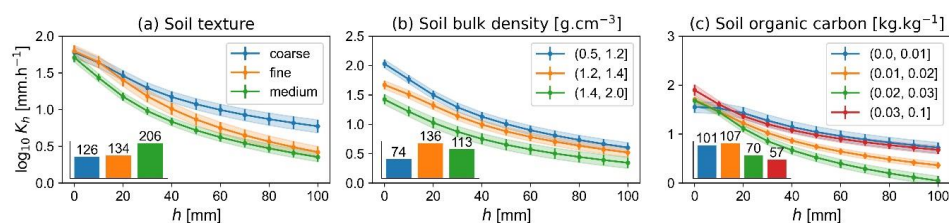
406

407 **Figure 7: Evolution of weighted mean K_h as a function of applied tension for (a) soil texture,**
408 **(b) soil bulk density and (c) soil organic carbon. The shaded areas and the error bars**
409 **represent the weighted standard error of the mean. The soil textures were classified using**
410 **USDA texture classes as follows: fine (clay, clay loam, silty clay, silty clay loam), medium**
411 **(silt loam, loam), coarse (loamy sand, sand, sandy clay, sandy clay loam, sandy loam). The**
412 **bar plots in each subplot indicate how many data points of each class were in the data set.**

413
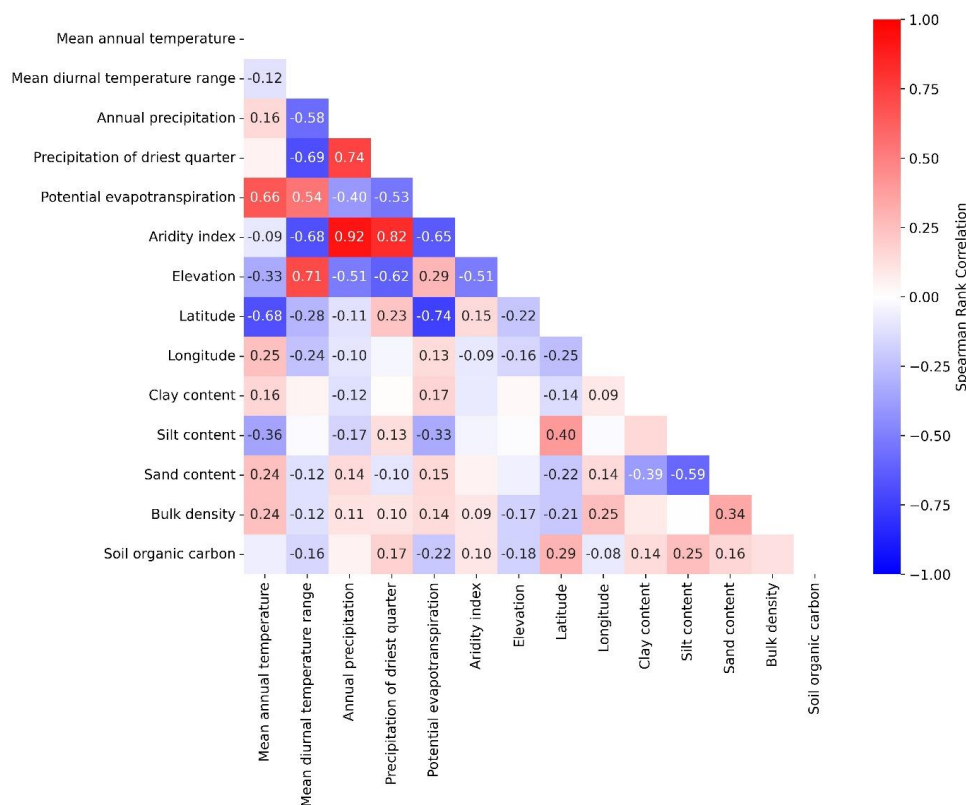
Table 5: Weighted Spearman rank correlation coefficients between climate variables, elevation above sea level and soil properties. Correlation coefficients are shown up to p-values of 0.001.

3.5   Statistical relationships between K_h and climate variables

One important observation made in recent years was that saturated and near-saturated hydraulic conductivities correlated strongly with climate variables (Jarvis et al., 2013; Jorda et al., 2015; Hirmas et al., 2018). Table 6 gives an overview of weighted Spearman rank correlations between K_h and six of the 20 climate variables included in OTIM that exhibited the strongest correlations with K_h. The elevation of the sampling site above sea level, its latitude and longitude, soil texture, bulk density and soil organic carbon content are also shown for comparison. It is striking that the soil properties were less well correlated with K_h than some of the climate variables. Of the three USDA texture fractions, the clay content was negatively and the sand content positively correlated with K_h at the drier investigated

426   tension range, while no significant correlations were found for the silt fraction (Table 6). Only the bulk

427   density exhibited correlation coefficients as large as the climate variables.

428   The largest absolute values of the weighted rank correlations were observed for the mean diurnal range

429   of temperature and the aridity index. Both reach a maximum at the dry end of the considered tension

430   range, i.e. for K_{100}, with correlation coefficients of 0.43 and -0.4, respectively. Table 5 reveals that both

431   of these best correlated climate variables were accidently correlated with choices in experimental

432   design and data evaluation made by the investigators in the respective source studies that will amplify

433   these observed correlations to K_h. However, if a smaller dataset is considered in which such

434   methodological bias as well as potential bias due to differences in land use were eliminated, the

435   correlations persisted (Table B1). We therefore infer that the observed effect of climate on K_h is real.
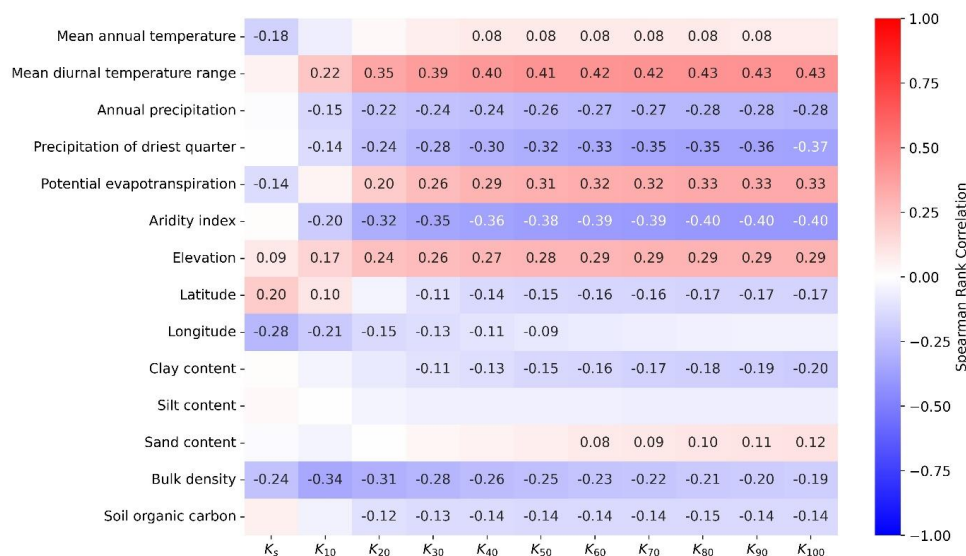
436

437   **Table 6: Weighted Spearman rank correlation coefficients between K_h at different tensions**

438   **and climatic features and soil properties. Correlation coefficients are shown up to p-values**

439   **of 0.001.**

440 The annual mean diurnal temperature range and the aridity index were strongly correlated with each

441 other, with a weighted correlation coefficient of -0.68 (Table 5). Strong correlations to at least one of

442 these two variables with absolute values >0.6 were also found for most of the investigated climate

443 variables. It is therefore difficult to separate the climate effects due to these strong inter-correlations.

444 Nevertheless, it is striking that the mean annual diurnal temperature ranges are much better correlated

445 with K_{100} than the mean annual temperature itself (Table 6). In addition, the mean annual precipitation

446 in the driest quarter of the year and the precipitation in the driest quarter of the year exhibited stronger

447 correlations than the mean annual precipitation. It appears that temperature and precipitation

448 fluctuations are more strongly coupled to near-saturated hydraulic conductivities than the absolute

449 temperatures or precipitation amounts.

450 Among possible reasons for the observed correlations may be increased splash erosion during heavy

451 rainfalls that are common in regions with large precipitation seasonality, more soil compaction in wetter

452 climates due to trafficking, a larger vertical burrowing activity of soil fauna in climates with large diurnal

453 temperature ranges, more vertically oriented root systems in arid climates or climate specific choices in

454 land use and soil management. The data in OTIM cannot provide an answer to these questions.

455 Investigations of such relationships should be the focus of future studies.

456 Another site factor that is positively correlated with K_h is the elevation above sea level (Table 6). Notably,

457 elevation above sea level also was found to be an important predictor for K_s in Gupta et al. (2021b),

458 which suggests that there are indeed pedogenetic reasons behind the observed correlation. In the case

459 of infiltrometer measurements, the decreased atmospheric pressure with height on the supply tension

460 can be neglected. The supply tension is always equivalent to the weight of the water column adjusted

461 in the bubbling tower. The weight of the water column will be smaller due to the general decrease of

462 earth's gravitational constant with height due to a larger centrifugal force. However, the weight of the

463 water column would only be reduced by approximately one or two percent. Also, indirect influences of

464 larger heights on the infiltration rate cannot explain the observed correlation. A lower temperature would

465 make the water column denser. However, the effect would be less than 1% in the relevant temperature

466 range. In contrast, a lower temperature would increase the viscosity of water to a much larger degree,

467   e.g. by up to approximately 30% between temperatures of 10 and 20 °C. The temperature effect should

468   thus lead to a negative correlation between elevation and K_h, which is the opposite of what was

469   observed. Bias in the K_h measurements due to such physical effects can thus be ruled out. Elevation

470   may instead be a proxy for well-drained soils, as stagnant soil water and high groundwater tables are

471   less likely with height above sea level. This may favour soil life and better developed root systems and

472   decrease risks of compaction when the soil is trafficked.

473   The observed correlations of K_h with latitude and longitude probably reflect co-correlations with climate

474   variables together with experimenter bias, since it appears likely that approaches in setting up tension

475   disk infiltrometers systematically vary between continents, e.g. America and Europe.

476   Bulk density was the only soil property that exhibited (negative) correlation strength of > 0.3 to any K_h

477   (Table 6). The underlying reasons have been discussed above. Notably, the strongest correlations were

478   found at and very close to saturation, probably due to the detrimental effect of soil compaction on

479   macroporosity and macropore connectivity. The more compaction, the less macroporosity remains and

480   the higher the bulk density, which in turn decreases root growth and bioturbation (Capowiez et al., 2021;

481   Lipiec and Hatano, 2003). The only pedo-climatic factor with relatively larger correlation strength (-0.31)

482   with the saturated hydraulic conductivity was the bulk density (Table 6).

3.6   Effects of land use, tillage, compaction and sampling time

484   The average log_{10} response ratios shown in Figure 8 illustrate the effects of land use and soil

485   management on K_h for $0 \leq h \leq 100$ mm. Note that a value of ±0.3 in the log_{10} response ratio corresponds

486   to a factor 2. Hence, K_s for uncompacted soil was found to be approximately twice as large as for

487   compacted soil (see Figure 8c). Arable land exhibited clearly smaller K_s than grasslands and forests,

488   which is in line with observations made by Basche & DeLonge, 2019. This difference became smaller

489   with higher tensions (Figure 8a). The large difference in K_h close to saturation was likely related to traffic

490   compaction as well as tillage operations that were applied to the majority of the investigated arable

491   soils, which lead to the destruction of connected biopores and hence a reduced K_s. On the other hand,

492   tillage breaks up intact soil into individual soil aggregates, which creates, at least initially, a well-

493   connected network of inter-aggregate pores that increase K_h in the near-saturated range (Sandin et al.,

494   2017; Schlüter et al., 2020). This effect of tillage can explain why near-saturated K_h under conventional

495   and reduced tillage was larger than under no-till (Figure 8b). However, in this case, even K_s was larger

496   in the tilled fields. It is likely that K_s was reduced in the no-till treatments due to traffic compaction on

497   the fields and a lack of soil loosening by tillage as compared to conventionally tilled treatments. Note

498   however, that we only investigated topsoils in this study. It is not clear that how different tillage types

499   affect K_h in the subsoil. The impact of soil compaction on K_h was clearly negative in the entire

500   investigated range of tensions (Figure 8c), which is explained by the reduction of porosity, and

501   especially the macroporosity during compaction (see also Figure 7b). In contrast, if the K_h

502   measurements were carried out shortly after tillage operations, K_h was increased for all investigated

503   tensions, especially very close to saturation (Figure 8d). This confirms that tillage initially increases K_s,

504   but that subsequent soil consolidation preferentially disconnects the largest macropores. As a

505   consequence, K_h at and very close to saturation is reduced more strongly than K_h for higher tensions.
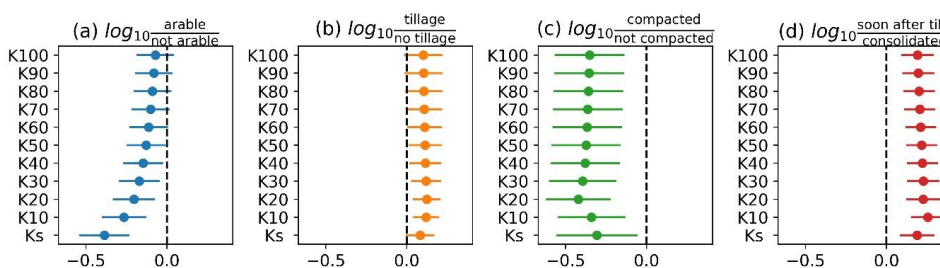
506

507   **Figure 8: Weighted mean $\log_{10}$ response ratio (effect size) of K_h for from K_{100} to K_s for**
508   **different management practises where the controls were 'not arable', 'no tillage', 'no**
509   **compaction' and 'consolidated soil' respectively. Positive effect size means that the value**
510   **of the treatment is greater than the control. Dashed line shows the "no effect" (no**
511   **difference between treatment and control). Error bars represent the weighted standard**
512   **error of the mean.**

513   Figure 9 shows the results of the sensitivity analyses for the effect sizes depicted in Figure 8. The effect

514   of land use for K_{100} turned out to be the most sensitive to the removal of studies (Figure 9a). The

515   direction of the effect even changed after removal of six studies, indicating that higher K_{100} for arable

516   compared to non-arable fields were not just occasional observations but occurred more frequently. More

517   studies would be needed to properly characterise the effect of land use on K_{100}. The remaining

518   sensitivity analyses for all the other factors showed that removal of studies did not change or destabilise

519   the results for both K_{100} and K_s.

520
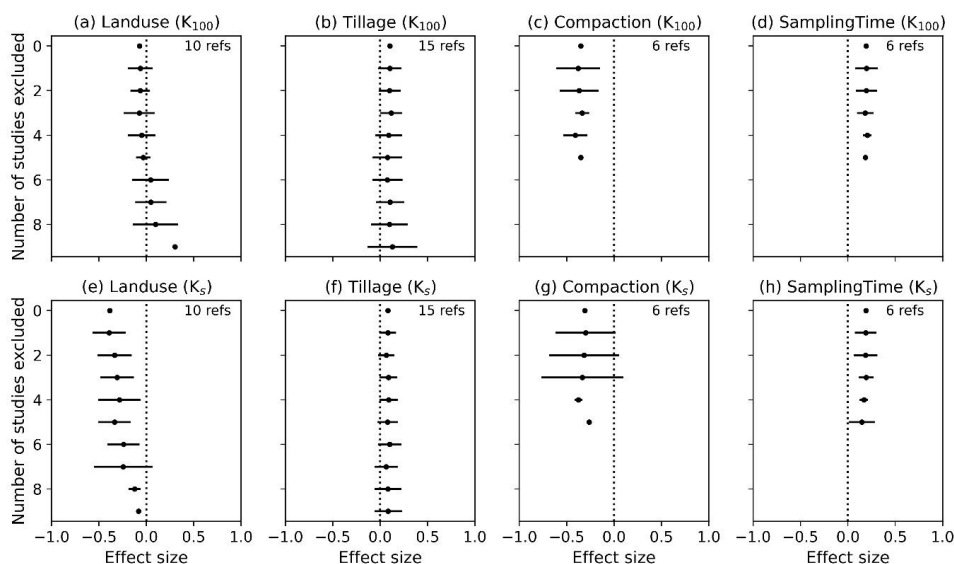
Figure 9: Sensitivity analysis of the weighted effect size of K at 100 mm tension and K_s for
the management practice investigated using the Jackknife technique. The error bars
represent the standard error.

3.7   Comparison of effect size of land use and management and sampling time with effect of climate and soil properties

526   Effect sizes could only be computed for land use and management, compaction as well as sampling

527   time. It is therefore difficult to relate the impact of these factors to the ones of measurement method,

528   climate variables and soil properties. Comparisons between figures 6, 7 and 10, on the one hand, with

529   Figure 8 provide some insight. Land use and management related effects and sampling time (Figure 8)

530   seem to have a similar effect on K_h as soil properties (Figure 7) and measurement method (Figure 6).

531   Climate variables seem to have a larger impact on K_h at the dry end of the investigated tension range,

532   but a smaller one close to saturation (Figure 10).

533
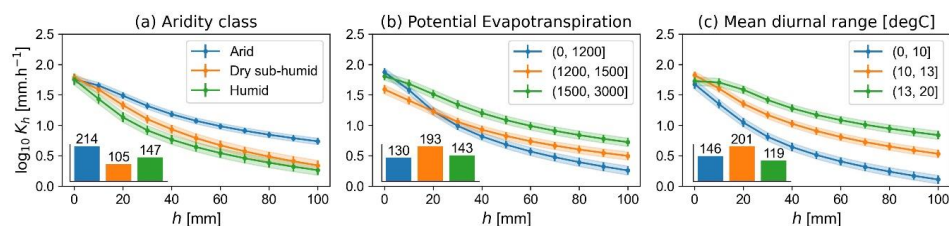
Figure 10: Evolution of weighted mean K_h as a function of applied tension for (a) aridity

class, (b) potential annual evapotranspiration and (c) mean annual diurnal temperature

range. The shaded areas and the error bars represent the weighted standard error of the

mean.

4   Conclusions

Our results suggest that climate change will influence soil hydraulic properties near saturation. This

may complicate model predictions of water balance in a future climate, particularly the risks of surface

runoff, soil erosion and waterlogging. Climatic factors are more strongly correlated to near-saturated

hydraulic conductivities than soil texture, bulk density and organic carbon content. At and very close to

soil saturation, the correlations between hydraulic conductivity and climate variables vanished,

indicating a change in flow paths. Instead, the soil bulk density showed the largest correlation, in line

with the fact that more compact soils tend to lack a well-connected macropore system. Hypotheses as

to why climate variables are correlated with the hydraulic conductivity were discussed, but these need

to be further investigated. Most probably, the impacts of climate are linked to macropore networks

associated with biological activity, pedogenesis, and land use. Only a few land use and soil

management related factors could be investigated in our study. They were all found to significantly

influence K_h, with effect sizes similar to those of soil properties like texture and organic carbon content.

Also, experimenter bias as introduced by choice of measurement time relative to soil tillage,

experimental design or data evaluation appeared to be as important for the saturated and near-

saturated hydraulic conductivity as soil texture or bulk density. There is a need for better documentation

554   and accessibility of measurement data and associated meta-data, as has already been suggested by

555   others (McBratney et al., 2011; Basche & DeLonge, 2019).

5   Appendix A

5.1   Data query details

Table A1: Query strings, search engines, number of result pages that were processed and

dates of the search for finding new data for OTIM

Search engine	Query string (time range considered)	Date	Pages
Google Scholar	hydraulic unsaturated conductivity tillage|crop	2021/06/02	12
Google Scholar	tension disk infiltrometer	2021/06/02	3
Web of Science	field unsaturated hydraulic conductivity agriculture	2021/06/02	3
Google Scholar	Near-saturated hydraulic conductivity (2013-2021)	2021/06/01	~8
ISI Web	Near-saturated hydraulic conductivity (2013-2021)	2021/06/01	~8
Scopus	Near-saturated hydraulic conductivity (2013-2021)	2021/06/01	~8
Google Scholar	hydraulic conductivity (2013-2021)	2021/05/31	~8
ISI Web	hydraulic conductivity (2013-2021)	2021/05/31	~8
Scopus	hydraulic conductivity (2013-2021)	2021/05/31	~8
Google Scholar	tension disk infiltrometer (2013-2021)	2021/05/31	~5
ISI Web	tension disk infiltrometer (2013-2021)	2021/05/31	~5
Google Scholar	Near-saturated hydraulic conductivity (2013-2021)	10/06/2021	~8
Google Scholar	tillage hydraulic conductivity (2013-2021)	10/06/2021	~8
Google Scholar	tension disk infiltrometer tillage (2013-2021)	10/06/2021	~8
Scopus	Near-saturated hydraulic conductivity (2013-2021)	10/06/2021	~3
Scopus	tillage hydraulic conductivity (2013-2021)	10/06/2021	~3
Scopus	tension disk infiltrometer (tillage) (2013-2021)	10/06/2021	~3
Scopus	"near-saturated" and infiltration	18/06/2021	~4
Scopus	"mini disk infiltrometer"	18/06/2021	~4
Scopus	"tension infiltrometer"	23/06/2021	~5

560

5.2   Data rejection

Table A2: Reasons for data rejection.

Reason	Number of publications
no access	2
not relevant	19

only one tension	61
overlap with another paper	3
no data published	32

563

5.3 Database organisation

565 OTIM is organised in nine individual tables illustrated in Table A3. The main table is named *experiments*.

566 It contains identifiers with which all the other tables are linked. The identifiers are shown in bold font in

567 Table A3. The *reference* table contains information on the references for each study. The *location* table

568 lists the coordinates of the measurement sites. The tables *soilProperties*, *soilManagement* and *climate*

569 store data as implied by their names. The *method* table gives details on the specifications of the tension-

570 disk infiltrometer and the method to calculate hydraulic conductivity from the infiltration rate. The

571 *rawData* table contains the hydraulic conductivities and respective supply tensions as stated in the

572 corresponding source publication. Note that OTIM does not contain raw data for the entries of the

573 original version compiled for Jarvis et al., 2013. Finally, *modelFit* reports K_h for $0 \le h \le 100$ mm as

574 described above. For more details, the reader is directed to the 'description' tab of the database (not

575 shown in Table A3) where the meanings and units of each column are explained.

576

577 **Table A3: Structure of the OTIM database with its different tables and columns. In the**
578 **_soilManagement_ table, the columns with the suffix "Class" denote columns in which the**
579 **data reported in the source publications were summarised into classes to facilitate**
580 **comparing them. For example, the reported _CurrentCrop_ like wheat, rye, barley or oat was**
581 **assigned the _CropClass_ cereals. The rows in bold denote unique identifiers with which the**
582 **table entries are linked to the _experiments_ table.**

583 # 6   Appendix B
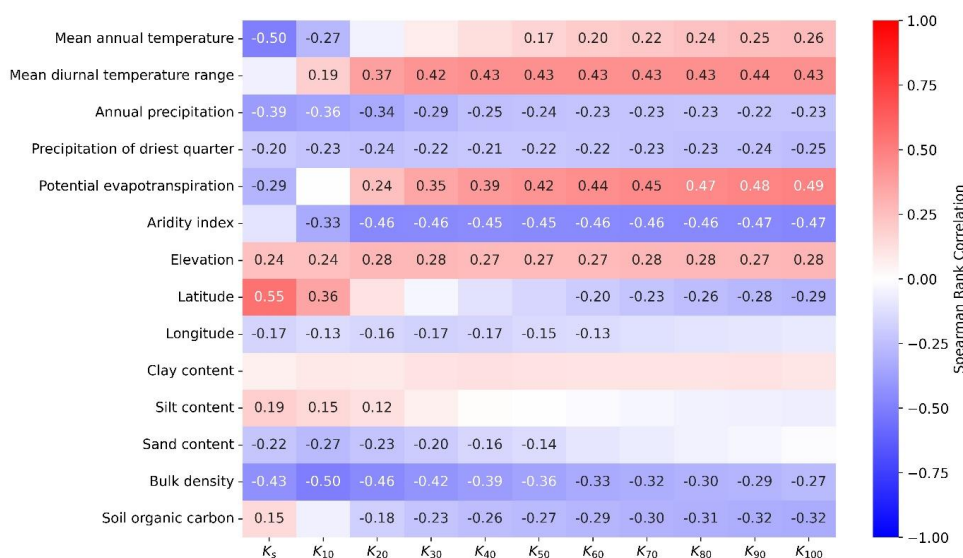
584

585 **Table B1: Weighted Spearman rank correlation coefficients between K_h at different**

586 **tensions and climatic features, soil properties, land use and management factors and**

587 **methodological details. In contrast to Table 6, only the 193 data entries from arable fields**

588 **using a dry-to-wet sequence and the steady-state piecewise method (Reynolds and Elrick,**

589 **1991; Ankeny et al., 1991) were considered. Correlation coefficients are shown up to p-**

590 **values of 0.001.**

591 # 7   Code availability

All scripts used to compile this study are publically available in form of Jupyter notebooks on GitHub:

https://github.com/climasoma/OTIM and https://github.com/climasoma/machine-learning.

8 Data availability

The OTIM database is available from the BONARES data repository https://tools.bonares.de/doi/datasets.

9 Author contribution

Funding acquisition: JK, SG; project administration, supervision and conceptualization: JK; meta-database collation and validation: LA, GuBl, JK; Python code development, including visualization: GuBl, JK; applying statistical analyses and writing original manuscript draft: GuBl, JK; Reviewing and editing the manuscript: JK, NJ, SG; GiBr, GuBl.

10 Competing interests

11 The authors declare that they have no conflict of interest.

12 Acknowledgements

This study was carried out in the framework of the EJP Soil ClimaSoMa project, which has received funding from the EU Horizon 2020 Research and Innovation programme under grant number 862695. We thank Lionel Alletto, Mats Larsbo, Ali Meshgi and Wim Cornelis for sharing additional details to their source publication.

13 References

Alagna, V., Bagarello, V., Di Prima, S., and Iovino, M.: Determining hydraulic properties of a loam soil by alternative infiltrometer techniques: Hydraulic Properties of a Loam Soil by Infiltrometer Techniques, Hydrol. Process., 30, 263–275, https://doi.org/10.1002/hyp.10607, 2016.

613   Alletto, L., Pot, V., Giuliano, S., Costes, M., Perdrieux, F., and Justes, E.: Temporal variation in soil

614   physical properties improves the water dynamics modeling in a conventionally-tilled soil, Geoderma,

615   243–244, 18–28, https://doi.org/10.1016/j.geoderma.2014.12.006, 2015.

616   Angulo-Jaramillo, R., Vandervaere, J. P., Roulier, S., Thony, J. L., Gaudet, J. P., and Vauclin, M.: Field

617   measurement of soil surface hydraulic properties by disc and ring infiltrometers - A review and recent

618   developments, Soil Tillage Res., 55, 1–29, 2000.

619   Ankeny, M. D., Ahmed, M., Kaspar, T. C., and Horton, R.: Simple field method for determining

620   unsaturated hydraulic conductivity, 55, 467–470, 1991.

621   Bagarello, V., Baiamonte, G., Castellini, M., Di Prima, S., and Iovino, M.: A comparison between the

622   single ring pressure infiltrometer and simplified falling head techniques: COMPARING PRESSURE

623   INFILTROMETER   AND   SFH   TECHNIQUES,   Hydrol.   Process.,   28,   4843–4853,

624   https://doi.org/10.1002/hyp.9980, 2014.

625   Baranian Kabir, E., Bashari, H., Bassiri, M., and Mosaddeghi, M. R.: Effects of land-use/cover change

626   on soil hydraulic properties and pore characteristics in a semi-arid region of central Iran, Soil and Tillage

627   Research, 197, 104478, https://doi.org/10.1016/j.still.2019.104478, 2020.

628   Basche, A. D. and DeLonge, M. S.: Comparing infiltration rates in soils managed with conventional and

629   alternative farming methods: A meta-analysis, 14, https://doi.org/10.1371/journal.pone.0215702, 2019.

630   Báťková, K., Miháliková, M., and Matula, S.: Hydraulic Properties of a Cultivated Soil in Temperate

631   Continental   Climate   Determined   by   Mini   Disk   Infiltrometer,   Water,   12,   843,

632   https://doi.org/10.3390/w12030843, 2020.

633   Bodner, G., Scholl, P., Loiskandl, W., and Kaul, H. P.: Environmental and management influences on

634   temporal   variability   of   near   saturated   soil   hydraulic   properties,   204,   120–129,

635   https://doi.org/10.1016/j.geoderma.2013.04.015, 2013.

636 Bottinelli, N., Menasseri-Aubry, S., Cluzeau, D., and Hallaire, V.: Response of soil structure and

637 hydraulic conductivity to reduced tillage and animal manure in a temperate loamy soil, Soil Use Manage,

638 29, 401–409, https://doi.org/10.1111/sum.12049, 2013.

639 Bouma, J.: Using soil survey data for quantitative land evaluation, 9, 177–213, 1989.

640 Capowiez, Y., Sammartino, S., Keller, T., and Bottinelli, N.: Decreased burrowing activity of endogeic

641 earthworms and effects on water infiltration in response to an increase in soil bulk density, Pedobiologia,

642 85-86, 150728, 2021.

643 Costa, J. L., Aparicio, V., and Cerdà, A.: Soil physical quality changes under different management

644 systems after 10 years in the Argentine humid pampa, Solid Earth, 6, 361–371,

645 https://doi.org/10.5194/se-6-361-2015, 2015.

646 De Boever, M., Gabriels, D., Ouessar, M., and Cornelis, W.: Influence of Acacia Trees on Near-Surface

647 Soil Hydraulic Properties in Arid Tunisia, Land Degrad. Develop., 27, 1805–1812,

648 https://doi.org/10.1002/ldr.2302, 2016.

649 Etana, A., Larsbo, M., Keller, T., Arvidsson, J., Schjønning, P., Forkman, J., and Jarvis, N.: Persistent

650 subsoil compaction and its effects on preferential flow patterns in a loamy till soil, Geoderma, 192, 430–

651 436, https://doi.org/10.1016/j.geoderma.2012.08.015, 2013.

652 Fashi, F. H., Gorji, M., and Sharifi, F.: THE USE OF SOIL HYDRAULIC PROPERTIES AS

653 INDICATORS FOR ASSESSING THE IMPACT OF MANAGEMENT PRACTICES UNDER SEMI-ARID

654 CLIMATES, Environ. Eng. Manag. J., 18, 1057–1066, https://doi.org/10.30638/eemj.2019.102, 2019.

655 Fasinmirin, J. T., Olorunfemi, I. E., and Olakuleyin, F.: Strength and hydraulics characteristics variations

656 within a tropical Alfisol in Southwestern Nigeria under different land use management, Soil and Tillage

657 Research, 182, 45–56, https://doi.org/10.1016/j.still.2018.04.017, 2018.

658 Greenwood: Land use and tillage effects on soil saturated hydraulic conductivity: Does infiltration

659 method matter?, Master Thesis, Lincoln University, New-Zeeland, 2017.

660 Fick, S. E. and Hijmans, R. J.: WorldClim 2: new 1-km spatial resolution climate surfaces for global land

661 areas, 37, 4302–4315, https://doi.org/10.1002/joc.5086, 2017.

662 Gupta, S., Hengl, T., Lehmann, P., Bonetti, S., and Or, D.: SoilKsatDB: global database of soil saturated

663 hydraulic conductivity measurements for geoscience applications, 13, 1593–1612,

664 https://doi.org/10.5194/essd-13-1593-2021, 2021a.

665 Gupta, S., Lehmann, P., Bonetti, S., Papritz, A., and Or, D.: Global Prediction of Soil Saturated

666 Hydraulic Conductivity Using Random Forest in a Covariate-Based GeoTransfer Function (CoGTF)

667 Framework, 13, e2020MS002242, https://doi.org/10.1029/2020MS002242, 2021b.

668 Hallam, J., Berdeni, D., Grayson, R., Guest, E. J., Holden, J., Lappage, M. G., Prendergast-Miller, M.

669 T., Robinson, D. A., Turner, A., Leake, J. R., and Hodson, M. E.: Effect of earthworms on soil physico-

670 hydraulic and chemical properties, herbage production, and wheat growth on arable land converted to

671 ley, Science of The Total Environment, 713, 136491, https://doi.org/10.1016/j.scitotenv.2019.136491,

672 2020.

673 Hardie, M. A., Doyle, R. B., Cotching, W. E., Mattern, K., and Lisson, S.: Influence of antecedent soil

674 moisture on hydraulic conductivity in a series of texture-contrast soils: INFLUENCE OF ANTECEDENT

675 SOIL MOISTURE ON HYDRAULIC CONDUCTIVITY, Hydrol. Process., 26, 3079–3091,

676 https://doi.org/10.1002/hyp.8325, 2012.

677 Hillel, D.: Introduction to Environmental Soil Physics, Academic Press, Amsterdam, 2004.

678 Hirmas, D. R., Giménez, D., Nemes, A., Kerry, R., Brunsell, N. A., and Wilson, C. J.: Climate-induced

679 changes in continental-scale soil macroporosity may intensify water cycle, 561, 100–103,

680 https://doi.org/10.1038/s41586-018-0463-x, 2018.

681 Holden, J., Wearing, C., Palmer, S., Jackson, B., Johnston, K., and Brown, L. E.: Fire decreases near-

682 surface hydraulic conductivity and macropore flow in blanket peat: FIRE AND BLANKET PEAT

683 HYDROLOGY, Hydrol. Process., 28, 2868–2876, https://doi.org/10.1002/hyp.9875, 2014.

684   Hyväluoma, J., Räty, M., Kaseva, J., and Keskinen, R.: Changes over time in near-saturated hydraulic

685   conductivity   of   peat   soil   following   reclamation   for   agriculture,   34,   237–243,

686   https://doi.org/10.1002/hyp.13578, 2020.

687   Iovino, M., Castellini, M., Bagarello, V., and Giordano, G.: Using Static and Dynamic Indicators to

688   Evaluate Soil Physical Quality in a Sicilian Area: SOIL PHYSICAL QUALITY EVALUATION BY STATIC

689   AND DYNAMIC INDICATORS, Land Degrad. Develop., 27, 200–210, https://doi.org/10.1002/ldr.2263,

690   2016.

691   IUSS Working Group WRB: World Reference Base for Soil Resources 2014, Update 2015. International

692   Soil Classification System for Naming Soils and Creating Legends for Soil Maps., FAO, Rome, 2015.

693   Jarvis, N., Koestel, J., Messing, I., Moeys, J., and Lindahl, A.: Influence of soil, land use and climatic

694   factors on the hydraulic conductivity of soil, 17, 5185–5195, https://doi.org/10.5194/hess-17-5185-2013,

695   2013.

696   Jorda, H., Bechtold, M., Jarvis, N., and Koestel, J.: Using boosted regression trees to explore key

697   factors   controlling   saturated   and   near-saturated   hydraulic   conductivity,   66,   744–756,

698   https://doi.org/10.1111/ejss.12249, 2015.

699   Kelishadi, H., Mosaddeghi, M. R., Hajabbasi, M. A., and Ayoubi, S.: Near-saturated soil hydraulic

700   properties as influenced by land use management systems in Koohrang region of central Zagros, Iran,

701   Geoderma, 213, 426–434, https://doi.org/10.1016/j.geoderma.2013.08.008, 2014.

702   Keskinen, R., Räty, M., Kaseva, J., and Hyväluoma, J.: Variations in near-saturated hydraulic

703   conductivity of arable mineral topsoils in south-western and central-eastern Finland, AFSci, 28,

704   https://doi.org/10.23986/afsci.79329, 2019.

705   Khetdan, C., Chittamart, N., Tawornpruek, S., Kongkaew, T., Onsamrarn, W., and Garré, S.: Influence

706   of rock fragments on hydraulic properties of Ultisols in Ratchaburi Province, Thailand, Geoderma

707   Regional, 10, 21–28, https://doi.org/10.1016/j.geodrs.2017.04.001, 2017.

708   Klute, A. and Dirksen, C.: Hydraulic conductivity and diffusivity: Laboratory measurements, in: Methods

709   of soil analysis, Part 1, vol. 1, edited by: Klute, A., Soil Science Society of America, Inc., Madison,

710   Wisconsin, USA, 687–734, 1986.

711   Koestel, J., Dathe, A., Skaggs, T. H., Klakegg, O., Ahmad, M. A., Babko, M., Giménez, D., Farkas, C.,

712   Nemes, A., and Jarvis, N.: Estimating the Permeability of Naturally Structured Soil From Percolation

713   Theory and Pore Space Characteristics Imaged by X-Ray, Water Resources Research, 54, 9255-9263,

714   2018.

715   Larsbo, M., Koestel, J., and Jarvis, N.: Relations between macropore network characteristics and the

716   degree of preferential solute transport, 18, 5255–5269, https://doi.org/10.5194/hess-18-5255-2014,

717   2014.

718   Larsbo, M., Sandin, M., Jarvis, N., Etana, A., and Kreuger, J.: Surface Runoff of Pesticides from a Clay

719   Loam Field in Sweden, J. Environ. Qual., 45, 1367–1374, https://doi.org/10.2134/jeq2015.10.0528,

720   2016a.

721   Larsbo, M., Koestel, J., Kätterer, T., and Jarvis, N.: Preferential transport in macropores is reduced by

722   soil organic carbon, Vadose Zone Journal, 15, 2016b.

723   Lipiec, J. and Hatano, R.: Quantification of compaction effects on soil physical properties and crop

724   growth, Geoderma, 116, 107-136, 2003.

725   Logsdon, S. D. and Jaynes, D. B.: Methodology for Determining Hydraulic Conductivity with Tension

726   Infiltrometers, 57, 1426–1431, https://doi.org/10.2136/sssaj1993.03615995005700060005x, 1993.

727   Lopes, V. S., Cardoso, I. M., Fernandes, O. R., Rocha, G. C., Simas, F. N. B., de Melo Moura, W.,

728   Santana, F. C., Veloso, G. V., and da Luz, J. M. R.: The establishment of a secondary forest in a

729   degraded pasture to improve hydraulic properties of the soil, Soil and Tillage Research, 198, 104538,

730   https://doi.org/10.1016/j.still.2019.104538, 2020.

731 Lozano, L. A., Germán Soracco, C., Buda, V. S., Sarli, G. O., and Filgueira, R. R.: Stabilization of soil

732 hydraulic properties under a long term no-till system, Rev. Bras. Ciênc. Solo, 38, 1281–1292,

733 https://doi.org/10.1590/S0100-06832014000400024, 2014.

734 Lozano-Baez, S. E., Cooper, M., Frosini de Barros Ferraz, S., Ribeiro Rodrigues, R., Castellini, M., and

735 Di Prima, S.: Assessing Water Infiltration and Soil Water Repellency in Brazilian Atlantic Forest Soils,

736 display, 2020.

737 Matula, S., Miháliková, M., Lufinková, J., and Báťková, K.: The role of the initial soil water content in the

738 determination of unsaturated soil hydraulic conductivity using a tension infiltrometer, Plant Soil Environ.,

739 61, 515–521, https://doi.org/10.17221/527/2015-PSE, 2015.

740 McBratney, A. B., Minasny, B., and Tranter, G.: Necessary meta-data for pedotransfer functions, 160,

741 627–629, https://doi.org/10.1016/j.geoderma.2010.09.023, 2011.

742 Meshgi, A. and Chui, T. F. M.: Analysing tension infiltrometer data from sloped surface using two-

743 dimensional approximation: ANALYSING TENSION INFILTROMETER DATA FROM SLOPED

744 SURFACE, Hydrological Processes, 28, 744–752, https://doi.org/10.1002/hyp.9621, 2014.

745 Messing, I. and Jarvis, N. J.: Seasonal variation in field-saturated hydraulic conductivity in two swelling

746 clay soils in Sweden, 41, 229–237, 1990.

747 Messing, I. & Jarvis, N.J.: Temporal variation in the hydraulic conductivity of a tilled clay soil as

748 measured by tension infiltrometers. Journal of Soil Science, 44, 11-24, 1993.

749 Meurer, K., Barron, J., Chenu, C., Coucheney, E., Fielding, M., Hallett, P., Herrmann, A. M., Keller, T.,

750 Koestel, J., Larsbo, M., Lewan, E., Or, D., Parsons, D., Parvin, N., Taylor, A., Vereecken, H., and Jarvis,

751 N.: A framework for modelling soil structure dynamics induced by biological activity, Glob. Change Biol.,

752 26, 5382–5403, https://doi.org/10.1111/gcb.15289, 2020.

753 Miller, J. J., Beasley, B. W., Drury, C. F., Larney, F. J., Hao, X., and Chanasyk, D. S.: Influence of long-

754 term feedlot manure amendments on soil hydraulic conductivity, water-stable aggregates, and soil

755   thermal properties during the growing season, Can. J. Soil. Sci., 98, 421–435,
756   https://doi.org/10.1139/cjss-2017-0061, 2018.

757   Nemes, A., Schaap, M. G., Leij, F. J., and Wosten, J. H. M.: Description of the unsaturated soil hydraulic
758   database UNSODA version 2.0, 251, 151–162, 2001.

759   Pagliai, M., Vignozzi, N., and Pellegrini, S.: Soil structure and the effect of management practices, Soil
760   & Tillage Research, 79, 131-143, 2004.

761   Poggio, L., de Sousa, L. M., Batjes, N. H., Heuvelink, G. B. M., Kempen, B., Ribeiro, E., and Rossiter,
762   D.: SoilGrids 2.0: producing soil information for the globe with quantified spatial uncertainty, SOIL, 7,
763   217-240, 2021.

764   Pulido Moncada, M., Helwig Penning, L., Timm, L. C., Gabriels, D., and Cornelis, W. M.: Visual
765   examinations and soil physical and hydraulic properties for assessing soil structural quality of soils with
766   contrasting textures and land uses, Soil and Tillage Research, 140, 20–28,
767   https://doi.org/10.1016/j.still.2014.02.009, 2014.

768   Rahbeh, M.: Characterization of preferential flow in soils near Zarqa river (Jordan) using in situ tension
769   infiltrometer measurements, 7, e8057, https://doi.org/10.7717/peerj.8057, 2019.

770   Rahmati, M., Weihermüller, L., Vanderborght, J., Pachepsky, Y. A., Mao, L., Sadeghi, S. H., Moosavi,
771   N., Kheirfam, H., Montzka, C., Van Looy, K., Toth, B., Hazbavi, Z., Al Yamani, W., Albalasmeh, A. A.,
772   Alghzawi, M. Z., Angulo-Jaramillo, R., Antonino, A. C. D., Arampatzis, G., Armindo, R. A., Asadi, H.,
773   Bamutaze, Y., Batlle-Aguilar, J., Béchet, B., Becker, F., Blöschl, G., Bohne, K., Braud, I., Castellano,
774   C., Cerdà, A., Chalhoub, M., Cichota, R., Císlerová, M., Clothier, B., Coquet, Y., Cornelis, W., Corradini,
775   C., Coutinho, A. P., De Oliveira, M. B., De Macedo, J. R., Durães, M. F., Emami, H., Eskandari, I.,
776   Farajnia, A., Flammini, A., Fodor, N., Gharaibeh, M., Ghavimipanah, M. H., Ghezzehei, T. A., Giertz,
777   S., Hatzigiannakis, E. G., Horn, R., Jiménez, J. J., Jacques, D., Keesstra, S. D., Kelishadi, H., Kiani-
778   Harchegani, M., Kouselou, M., Jha, M. K., Lassabatere, L., Li, X., Liebig, M. A., Lichner, L., López, M.
779   V., Machiwal, D., Mallants, D., Mallmann, M. S., De Oliveira Marques, J. D., Marshall, M. R., Mertens,

780   J., Meunier, F., Mohammadi, M. H., Mohanty, B. P., Pulido-Moncada, M., Montenegro, S., Morbidelli,

781   R., Moret-Fernández, D., Moosavi, A. A., Mosaddeghi, M. R., Mousavi, S. B., Mozaffari, H., Nabiollahi,

782   K., Neyshabouri, M. R., Ottoni, M. V., Ottoni Filho, T. B., Pahlavan-Rad, M. R., Panagopoulos, A., Peth,

783   S., Peyneau, P. E., Picciafuoco, T., Poesen, J., Pulido, M., Reinert, D. J., Reinsch, S., Rezaei, M.,

784   Roberts, F. P., Robinson, D., Rodrigo-Comino, J., Rotunno Filho, O. C., Saito, T., et al.: Development

785   and analysis of the Soil Water Infiltration Global database, 10, 1237–1263, https://doi.org/10.5194/essd-

786   10-1237-2018, 2018.

787   Reynolds, W. D. and Elrick, D. E.: Determination of Hydraulic Conductivity Using a Tension Infiltrometer,

788   55, 633–639, https://doi.org/10.2136/sssaj1991.03615995005500030001x, 1991.

789   Rienzner, M. and Gandolfi, C.: Investigation of spatial and temporal variability of saturated soil hydraulic

790   conductivity   at   the   field-scale,   Soil   and   Tillage   Research,   135,   28–40,

791   https://doi.org/10.1016/j.still.2013.08.012, 2014.

792   Sandin, M., Koestel, J., Jarvis, N., and Larsbo, M.: Post-tillage evolution of structural pore space and

793   saturated   and   near-saturated   hydraulic   conductivity   in   a   clay   loam   soil,   165,   161–168,

794   https://doi.org/10.1016/j.still.2016.08.004, 1, 2017.

795   Schaap, M. G. and Leij, F. J.: Improved prediction of unsaturated hydraulic conductivity with the

796   Mualem-van Genuchten model, Soil Science Society of America Journal, 64 (3), pp. 843 – 851, 2000.

797   Schaap, M. G., Leij, F. J., and van Genuchten, M. T.: ROSETTA: a computer program for estimating

798   soil hydraulic parameters with hierarchical pedotransfer functions, Journal of Hydrology, 251, 163–176,

799   2001.

800   Schlüter, S., Albrecht, L., Schwärzel, K., and Kreiselmeier, J.: Long-term effects of conventional tillage

801   and no-tillage on saturated and near-saturated hydraulic conductivity – Can their prediction be improved

802   by pore metrics obtained with X-ray CT? Geoderma, 361, 2020.

803   Smettem, K. R. J. and Clothier, B. E.: Measuring unsaturated sorptivity and hydraulic conductivity using

804   multiple disc permeameters, 40, 563–568, https://doi.org/10.1111/j.1365-2389.1989.tb01297.x, 1989.

805   Soracco, C. G., Lozano, L. A., Villarreal, R., Palancar, T. C., Collazo, D. J., Sarli, G. O., and Filgueira,

806   R. R.: EFFECTS OF COMPACTION DUE TO MACHINERY TRAFFIC ON SOIL PORE

807   CONFIGURATION,   Rev.   Bras.   Ciênc.   Solo,   39,   408–415,

808   https://doi.org/10.1590/01000683rbcs20140359, 2015.

809   Soracco, C. G., Villarreal, R., Melani, E. M., Oderiz, J. A., Salazar, M. P., Otero, M. F., Irizar, A. B., and

810   Lozano, L. A.: Hydraulic conductivity and pore connectivity. Effects of conventional and no-till systems

811   determined   using   a   simple   laboratory   device,   Geoderma,   337,   1236–1244,

812   https://doi.org/10.1016/j.geoderma.2018.10.045, 2019.

813   Tóth, B., Weynants, M., Nemes, A., Makó, A., Bilas, G., and Tóth, G.: New generation of hydraulic

814   pedotransfer functions for Europe, 66, 226–238, https://doi.org/10.1111/ejss.12192, 2015.

815   Trabucco, A. and Zomer, R.: Global Aridity Index and Potential Evapotranspiration (ET0) Climate

816   Database, https://doi.org/10.6084/m9.figshare.7504448.v3, 2019.

817   Van Looy, K., Bouma, J., Herbst, M., Koestel, J., Minasny, B., Mishra, U., Montzka, C., Nemes, A.,

818   Pachepsky, Y. A., Padarian, J., Schaap, M. G., Toth, B., Verhoef, A., Vanderborght, J., van der Ploeg,

819   M. J., Weihermuller, L., Zacharias, S., Zhang, Y. G., and Vereecken, H.: Pedotransfer Functions in

820   Earth   System   Science: Challenges   and   Perspectives,   55,   1199–1256,

821   https://doi.org/10.1002/2017rg000581, 2017.

822   Vandervaere, J.-P., Vauclin, M., and Elrick, D. E.: Transient Flow from Tension Infiltrometers II. Four

823   Methods   to   Determine   Sorptivity   and   Conductivity,   64,   1272–1284,

824   https://doi.org/10.2136/sssaj2000.6441272x, 2000.

825   Vereecken, H., Weynants, M., Javaux, M., Pachepsky, Y., Schaap, M. G., and Genuchten, M. T. v.:

826   Using pedotransfer functions to estimate the van Genuchten–Mualem soil hydraulic properties: A

827   review, Vadose Zone Journal, 9, 795-820, 2010.

828   Wang, L., Garré, S., De Cuypere, T., Pollet, S., Cornelis, W. unpublished data.

829 Wanniarachchi, D., Cheema, M., Thomas, R., Kavanagh, V., and Galagedara, L.: Impact of Soil
830 Amendments on the Hydraulic Conductivity of Boreal Agricultural Podzols, Agriculture, 9, 133,
831 https://doi.org/10.3390/agriculture9060133, 2019.

832 Weynants, M., Vereecken, H., and Javaux, M.: Revisiting Vereecken pedotransfer functions:
833 Introducing a closed-form hydraulic model, 8, 86–95, https://doi.org/10.2136/vzj2008.0062, 2009.

834 Weynants, M., Montanarella, L., Toth, G., Arnoldussen, A., Anaya Romero, M., Bilas, G., Borresen, T.,
835 Cornelis, W., Daroussin, J., Feichtinger, F., Gonçalves, M., Hannam, J., Haugen, L., Hennings, V.,
836 Houskova, B., Iovino, M., Javaux, M., Keay, C., Kätterer, T., Kvaerno, S., Laktinova, T., Lamorski, K.,
837 Lilly, A., Mako, A., Matula, S., Morari, F., Nemes, A., Nyborg, Å., Patyka, N., Riley, H., Romano, N.,
838 Schindler, U., Shein, E., Slawinski, C., Strauss, P., Tóth, B., and Woesten, H.: European
839 HYdropedological Data Inventory (EU-HYDI). EUR 26053, Publications Office of the European Union,
840 Luxembourg (Luxembourg). JRC81129., 2013.

841 Whalley, W. R., Dumitru, E., and Dexter, A. R.: Biological effects of soil compaction, Soil and Tillage
842 Research, 35, 53-68, 1995.

843 Wösten, J. H. M., Lilly, A., Nemes, A., and le Bas, C.: Development and use of a database of hydraulic
844 properties of European soils, 90, 169–185, 1999.

845 Wösten, J. H. M., Pachepsky, Y. A., and Rawls, W. J.: Pedotransfer functions: bridging the gap between
846 available basic soil data and missing soil hydraulic characteristics, 251, 123–150,
847 https://doi.org/10.1016/S0022-1694(01)00464-4, 2001.

848 Wooding, R. A.: Steady Infiltration from a Shallow Circular Pond, Water Resources Research, 4, 1259-
849 1273, 1968.

850 Yu, Z., Dong, W., Young, M. H., Li, Y., and Yang, T.: On evaluating characteristics of the solute transport
851 in the arid vadose zone, 52, 50–62, https://doi.org/10.1111/gwat.12026, 2014.

852 Yusuf, K. O., Ejieji, C. J., and Baiyeri, M. R.: Determination of sorptivity, infiltration rate and hydraulic

853 conductivity of soil using a tension infiltrometer, 10, 99–108, 2018.

854 Yusuf, K. O., Obalowu, R. O., Akinleye, G. T., and Adio-Yusuf, S. I.: Determination of Sorptivity,

855 Infiltration Rate and Hydraulic Conductivity of Loamy Sand using Tension Infiltrometer and Double-Ring

856 Infiltrometer, FUOYEJET, 5, https://doi.org/10.46792/fuoyejet.v5i2.501, 2020.

857 Zeng, C., Zhang, F., Wang, Q., Chen, Y., and Joswiak, D. R.: Impact of alpine meadow degradation on

858 soil hydraulic properties over the Qinghai-Tibetan Plateau, Journal of Hydrology, 478, 148–156,

859 https://doi.org/10.1016/j.jhydrol.2012.11.058, 2013a.

860 Zeng, C., Wang, Q., Zhang, F., and Zhang, J.: Temporal changes in soil hydraulic conductivity with

861 different soil types and irrigation methods, Geoderma, 193–194, 290–299,

862 https://doi.org/10.1016/j.geoderma.2012.10.013, 2013b.

863 Zhang, R.: Determination of Soil Sorptivity and Hydraulic Conductivity from the Disk Infiltrometer, 61,

864 1024–1030, https://doi.org/10.2136/sssaj1997.03615995006100040005x, 1997.

865 Zhang, Y., Zhao, W., Li, X., Jia, A., and Kang, W.: Contribution of soil macropores to water infiltration

866 across different land use types in a desert–oasis ecoregion, Land Degrad Dev, 32, 1751–1760,

867 https://doi.org/10.1002/ldr.3823, 2021.

868 Zhang, Z., Lin, L., Wang, Y., and Peng, X.: Temporal change in soil macropores measured using tension

869 infiltrometer under different land uses and slope positions in subtropical China, J Soils Sediments, 16,

870 854–863, https://doi.org/10.1007/s11368-015-1295-z, 2016.

871 Zhang, Z. B., Zhou, H., Zhao, Q. G., Lin, H., and Peng, X.: Characteristics of cracks in two paddy soils

872 and their impacts on preferential flow, Geoderma, 228–229, 114–121,

873 https://doi.org/10.1016/j.geoderma.2013.07.026, 2014.

874   Zhang, Z.-H., Li, X.-Y., Jiang, Z.-Y., Peng, H.-Y., Li, L., and Zhao, G.-Q.: Changes in some soil

875   properties induced by re-conversion of cropland into grassland in the semiarid steppe zone of Inner

876   Mongolia, China, Plant Soil, 373, 89–106, https://doi.org/10.1007/s11104-013-1772-3, 2013.

877   Zhao, X., Wu, P., Gao, X., Tian, L., and Li, H.: Changes of soil hydraulic properties under early-stage

878   natural vegetation recovering on the Loess Plateau of China, CATENA, 113, 386–391,

879   https://doi.org/10.1016/j.catena.2013.08.023, 2014.

880   Zhou, B. B., Wang, Q. J., and Wu, X. B.: Optimal disc tension infiltrometer estimation techniques for

881   hydraulic   properties   of   soil   under   different   land   uses,   9,   92–98,

882   https://doi.org/10.3965/j.ijabe.20160904.2161, 2016.

883   کریمییان, ن.: اثر روشهای خاکورزی و مدیریت بقایای گیاهی and ., میرزاوند, ج., موسوی, س. ع. ا., ثامنی, ع., افضلی نیا, ص

884   , برهدایت هیدرولیکی غیر اشباع خاک در تناوب گندم – ذرت, مجله پژوهشهای حفاظت آب و خاک, 23

885   https://doi.org/10.22069/jwfst.2016.3190, 2016.